

Microstructure, Interface Morphology, and Antioxidant Properties of Sn-8.5Zn-0.1Cr-(Nd,Al,Cu) Solders

HONGQUN TANG,¹ MOUMIAO LIU,¹ YUEYUAN MA,¹ ZAIXIANG DU,¹
YONGZHONG ZHAN,^{1,2} and WENCHAO YANG^{1,3}

1.—College of Materials Science and Engineering, Guangxi University, Nanning 530004, Guangxi, People's Republic of China. 2.—e-mail: zyzmatres@163.com. 3.—e-mail: ywc053@163.com

The effects of minor alloying element Nd, Al or Cu on the fundamental microstructural properties, interface morphology, and antioxidant properties of Sn-8.5Zn-0.1Cr (SZC) alloy have been investigated. Addition of Nd, Al or Cu element significantly refined the microstructure of SZC alloy, especially promoting disappearance of the stripe Zn-rich phase. Precipitated phases could be found in the β -Sn matrix when the content of each element reached 0.1 wt.%. During soldering, it was found that Nd, Al or Cu element addition did not contribute to intermetallic compound (IMC) formation, as verified by the same IMC phase as at the Sn-8.5Zn/Cu interface and no obvious influence on interface morphology. After 15 days of aging, IMC interface layers increased severely and a wide Zn-poor transition zone formed. The growth rate of IMC was reduced and the transition zone became narrower after microalloying. Meanwhile, addition of Al or Cu element improved the oxidation resistance of the SZC alloy, while Nd-containing alloys oxidized severely. The wettability and microhardness of the SZC-*x*M alloys were superior to those of SZC alloy.

Key words: Lead-free solder, microstructure, interface, antioxidant properties

INTRODUCTION

With the development of society, the limitations of traditional Sn-Pb solders have become more prominent. Research and development into lead-free solders is an irresistible trend. Due to their low melting point, moderate cost, good mechanical performance, etc., Sn-Zn-based lead-free solders are considered to be some of the most promising materials to replace traditional lead solders. However, owing to the presence of active zinc, Sn-Zn-based lead-free solders are easily oxidized, leading to poor wetting and antioxidant abilities.¹

There are two methods to improve the wettability of Sn-Zn solders: development of new kinds of flux suitable for Sn-Zn lead-free solders, and improvement of the oxidation resistance by microalloying.² In recent years, the alloying method has been widely adopted. Alloying elements such as Nd, Al,

Cu, Cr, etc. have been used to improve the mechanical and antioxidation properties of Sn-Zn solders. Hu et al.^{3,4} considered that rare-earth element Nd could remarkably improve the solderability and mechanical properties of Sn-9Zn solder joints, and also improve the oxidation resistance of Sn-9Zn solder. However, Zhou et al.⁵ showed that solely adding Nd element to Sn-Zn alloy had no positive impact on the antioxidant properties. Inclusion of an appropriate amount of Al element is highly beneficial to the wetting and antioxidant abilities of Sn-Zn alloy.^{6–8} Addition of Cu element can decrease the activity of Zn atoms, improving the wetting property and oxidation resistance.^{9,10} It was reported that Cr element not only favors oxidation resistance but also results in good performance in terms of mechanical properties.^{2,11,12} Based on previous studies,^{11,12} Sn-8.5Zn-0.1Cr was selected as the matrix alloy in this work.

The main objective of this work is to demonstrate the effect of Nd, Al or Cu additive on the

microstructure, wettability, oxidation resistance, and microhardness of Sn-8.5Zn-0.1Cr alloy, and determine the optimum composition to improve its performance.

EXPERIMENTAL PROCEDURES

Sn-8.5Zn-0.1Cr- x M solder alloys ($M = \text{Nd, Al, Cu}$; $x = 0 \text{ wt.}\%$, $0.05 \text{ wt.}\%$, $0.1 \text{ wt.}\%$) were investigated in this work. A series of pure metals (greater than 99.9% purity) were prepared. Due to the problem of high melting point, the master alloy method was used in this work to prepare the solder alloys. Firstly, Sn-5Cr, Sn-5Nd, Sn-5Al, and Sn-10Cu master alloys were prepared in vacuum arc furnace under Ar atmosphere. Secondly, the prepared master alloys together with Zn and Sn were mixed and melted in a box-type resistance furnace at 580°C . The molten solder in the ceramic crucible was poured into a prepared iron mold at 350°C . To prevent oxidation of elements, KCl-LiCl melting salt was used in the smelting process.

The melting behavior of the alloys was evaluated by differential scanning calorimetry (DSC). Solder (20 mg) was heated at rate of $10^\circ\text{C min}^{-1}$ up to 300°C under Ar atmosphere. The antioxidant properties of the alloys were evaluated by thermogravimetric analysis (TGA). Solder (20 mg) was heated at rate of $10^\circ\text{C min}^{-1}$ up to 250°C under air atmosphere and kept for 30 min. For observation of surface gloss, samples were processed into squares with 1.5 mm thickness and cleaned in ethanol after polishing. Solder sheets placed in ceramic crucibles were isothermally aged in a resistance furnace at 250°C for 1 h, 24 h, and 72 h, then the surface gloss of the samples was recorded using a digital camera. Evaluation of the wetting property was investigated by spreading test. The experimental substrates were copper (99.9% purity) cut to size of $30 \text{ mm} \times 30 \text{ mm} \times 0.1 \text{ mm}$, then degreased in 10% HCl solution and cleaned in ethanol after polishing. Solder (0.2 g) was processed into solder ball and placed on Cu substrate with $\text{ZnCl}_2\text{-NH}_4\text{Cl}$ flux, kept for 120 s at 250°C in a furnace, then cooled in air. The microhardness of the alloy was measured using an HVT-1000-type microhardness tester. Because the microhardness of the solder was relatively low, the experimental force used was 0.98 N and the retention time was 10 s. The samples were measured repeatedly in different regions, and the average value for each sample was taken as the microhardness value.

Soldered Cu samples were isothermally aged in a furnace at 150°C for 4 days and 15 days. The interface morphology was observed in cross-sections of these specimens. The microstructure and interface morphology were investigated by scanning electron microscopy (SEM) and energy-dispersive spectroscopy (EDS).

RESULTS AND DISCUSSION

Microstructural Characterization of Sn-Zn-Cr-M Alloys

Figure 1 shows SEM images of Sn-8.5Zn and SZC alloys. As shown in Fig. 1a, the microstructure of the Sn-8.5Zn solder alloy consisted of β -Sn matrix phase, rod- or needle-like Zn-rich phase, and eutectic structures. Figure 1b shows the microstructure of SZC solder. With addition of Cr, the needle-like Zn-rich phase decreased and a second phase precipitated. In previous work, the second phase in SZC alloy was confirmed to be Cr_2Sn_3 . On the one hand, Cr solution in the matrix of Sn-8.5Zn alloy results in solution strengthening; on the other hand, the second phase can increase the heterogeneous nucleation process, which is the reason for grain refinement.

With addition of Nd, Al or Cu, the microstructure of the SZC alloy changed in two aspects: transformation of Zn-rich structures, and formation of new phase.

With Nd addition, the needle-like Zn-rich phase decreased and became smaller, while the eutectic structure was enhanced, as shown in Fig. 2. According to the theory of metal solidification, surface-active elements such as Nd gather in front of the solid-liquid interface and increase the degree of

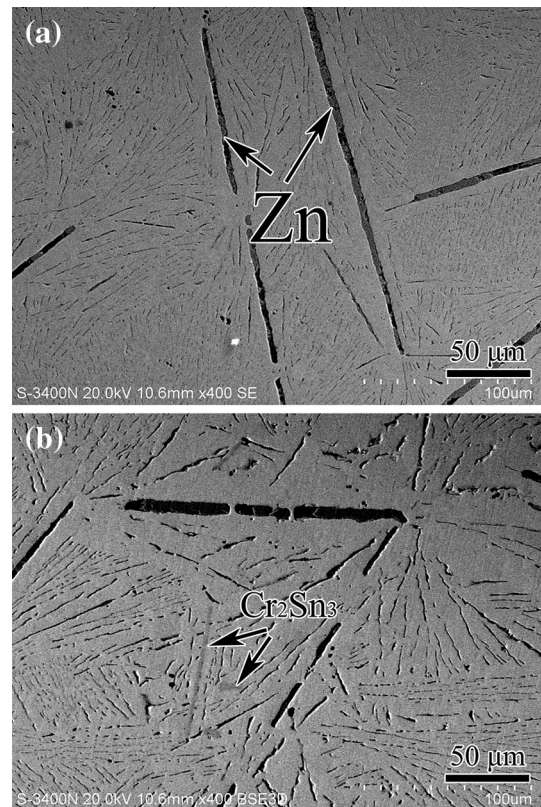


Fig. 1. Microstructure of (a) Sn-8.5Zn and (b) SZC alloys.

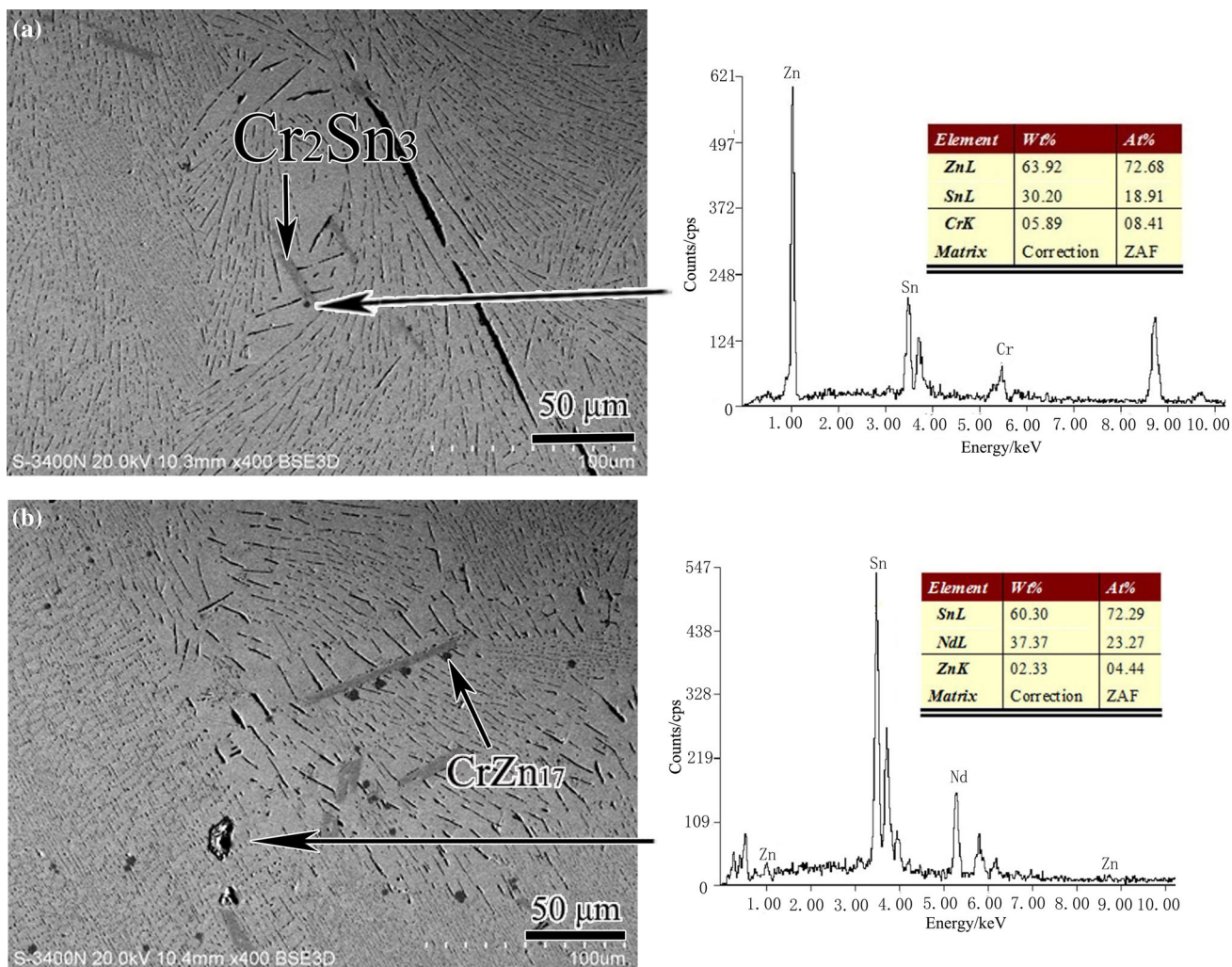


Fig. 2. Microstructure and EDS of SZC-*x*Nd alloys: (a) SZC-0.05Nd and (b) SZC-0.1Nd.

compositional supercooling, causing the grain growth pattern to transform from flat to cellular. So, Zn-rich phase and eutectic structure can be refined by adding Nd. A new black phase formed in the matrix when Nd was added to SZC alloy, as shown in Fig. 2a and b. The new phase can be speculated to be a Cr-Zn phase besides Cr₂Sn₃, being composed of 72.68Zn, 18.91Sn, 8.41Cr (at.%) according to EDS. Luo et al.¹³ found CrZn₁₇ phase in Sn-Zn-Bi-Cr lead-free solder. Because the atomic percentages for CrZn₁₇ are similar to our EDS results, we deduce the new phase to be CrZn₁₇. Such precipitation of CrZn₁₇ phase in SZC alloy shows that addition of Nd element can promote combination of Cr with Zn, thus reducing the possibility of oxidation of free-state Zn during the welding process. When the Nd content was 0.1 wt.%, a new phase formed, as seen in Fig. 2b. The black island phase in SZC-0.1Nd alloy was proved to be NdSn₃ based on the Sn-Nd binary phase diagram and energy-dispersive spectroscopy (EDS) analysis

(Fig. 2b). NdSn₃ phase is a hard brittle phase, so massive NdSn₃ phase is not favorable for the mechanical properties of the alloy.

Figure 3 shows the change in the microstructure after Al addition to the SZC alloy. Figure 3 shows that the Zn-rich phase decreased while the eutectic structure became finer, too. The mechanism of Al in SZC is similar to that of Nd, but there was no new phase with addition of more Al, in contrast to Cai's¹⁴ work.

When Cu was added to the SZC alloy, decreased Zn-rich phase and finer eutectic were obvious (Fig. 4), as well as CrZn₁₇ phase. The main reason for the refined structures is that, with Cu addition, Zn element tends to combine with Cu to produce Cu-Zn compound, which can play a role in heterogeneous nucleation. In Fig. 4b, the small black granular phase in the SZC-0.1Cu alloy is proved to be Cu₅Zn₈ phase by EDS analysis.

In conclusion, addition of Nd, Al or Cu can refine the microstructure of SZC alloy, especially the long

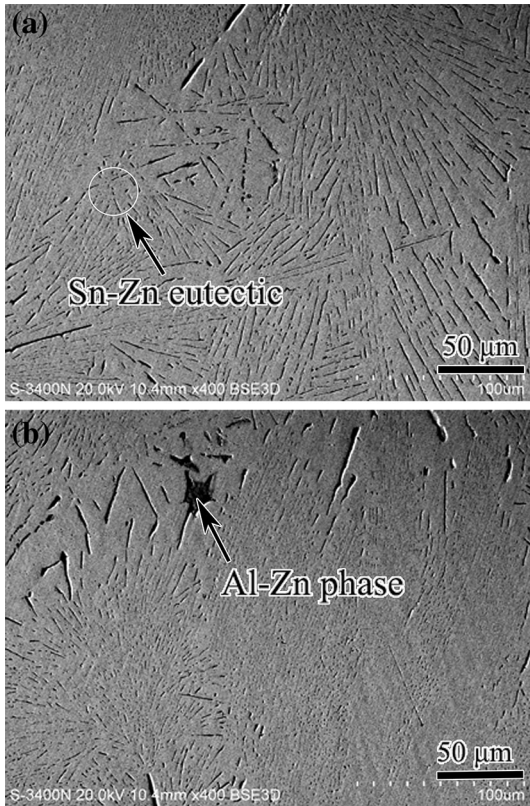


Fig. 3. Microstructure of SZC-*x*Al alloys: (a) SZC-0.05Al and (b) SZC-0.1Al.

stripes of Zn-rich phase, and can promote precipitation of CrZn_{17} phase to reduce the activity of Zn element. When the content of Nd, Al or Cu is 0.1 wt.%, some new phases form. According to EDS analysis, massive precipitation of NdSn_3 phase occurs in SZC-0.1Nd alloy, precipitation of Al-Zn butterfly crystal occurs in SZC-0.1Al alloy, and small granular Cu_5Zn_8 phase in SZC-0.1Cu alloy.

Melting Characteristics of Sn-Zn-Cr-M Alloys

DSC analysis was carried out to investigate the fundamental thermal reactions on heating the alloys. Figure 5 shows typical DSC curves obtained for Sn-8.5Zn and SZC-*x*M alloys on heating. Relevant parameters of the DSC analysis of SZC-*x*M alloys are listed in Table I.

Addition of small amount of Nd, Al or Cu element resulted in only slight change of the melting temperature compared with the value of 198.76°C for Sn-8.5Zn alloy but had a great influence on the melting temperature range of the alloys, as shown in Table I. With addition of Nd, β -Sn had more nucleation particles during solidification and the nucleation rate increased.¹⁵ This is the reason why addition of Nd element could reduce the melting temperature range. The melting temperature range was 5.16°C and 6.37°C for SZC-0.05Al and SZC-0.1Al alloy, respectively. The melting temperature

range was obviously decreased. Sebaoun et al.¹⁶ reported that Al, Sn, and Zn can form a solid solution, and the eutectic point is only 197°C. This is a reason why Al element could reduce the melting temperature range. This was also proven in earlier study by Das et al.⁶ The melting temperature range was 8.84°C and 9.02°C for SZC-0.05Cu and SZC-0.1Cu alloy, respectively. Addition of Cu element slightly decreased the melting temperature range. Yu et al.¹⁰ also reported that addition of a small amount of Cu did not significantly influence the melting behavior of Sn-9Zn alloy.

Oxidation Behavior of Sn-Zn-Cr-M Alloys

Table II presents the appearance of the alloys after different heating times at 250°C. As seen from Table II, during the period of heating, the color of the alloy surface went from silvery white to faint yellow, then turned gray, finally gradually turning black and losing its metallic luster. This is caused by oxidation of the metal surface elements. Compared with Sn-8.5Zn alloy, the surface gloss of SZC, SZC-Al, and SZC-Cu alloys was bright, while the surface gloss of SZC-Nd clearly turned black. This shows that adding Al or Cu element could contribute to the antioxidant properties, while addition of Nd element would deteriorate the antioxidant properties. SZC-0.05Al exhibited the best antioxidant properties in this work.

However, surface gloss observation experiments cannot accurately determine the antioxidant properties of alloys. In this work, the thermogravimetric analysis (TGA) method was adopted to characterize the antioxidant properties with added Nd, Al or Cu element.

The curves in Fig. 6 show how the weight of the Sn-8.5Zn and SZC-*x*M alloys changed with time under heating, namely TGA curves. In TGA curves, the oxidation weight was used to measure the maintenance or deterioration of the antioxidant properties. As shown in Fig. 6, the resulting antioxidant ability of the alloys lay in the following order (from strong to weak): SZC-0.05Al, SZC-0.1Al, SZC-0.1Cu, SZC-0.05Cu, SZC, Sn-8.5Zn, SZC-0.05Nd, SZC-0.1Nd.

From the perspective of the capacity of the alloy elements and oxygen to combine, the electronegativity difference between the alloy elements and oxygen is an important parameter. When the electronegativity difference between two elements is larger, a stable compound is easier to obtain. Table III presents the electronegativity difference between some elements and oxygen. Compared with Zn and O, the electronegativity difference between Cr and O is slightly smaller. In the molten state of SZC alloy, Zn will preferentially engage in surface oxidation while Cr element will tend to gather in the subsurface of the alloy liquid to form a protective layer preventing further oxygen diffusion. Huang et al.¹⁷ also reported a similar finding and proved its

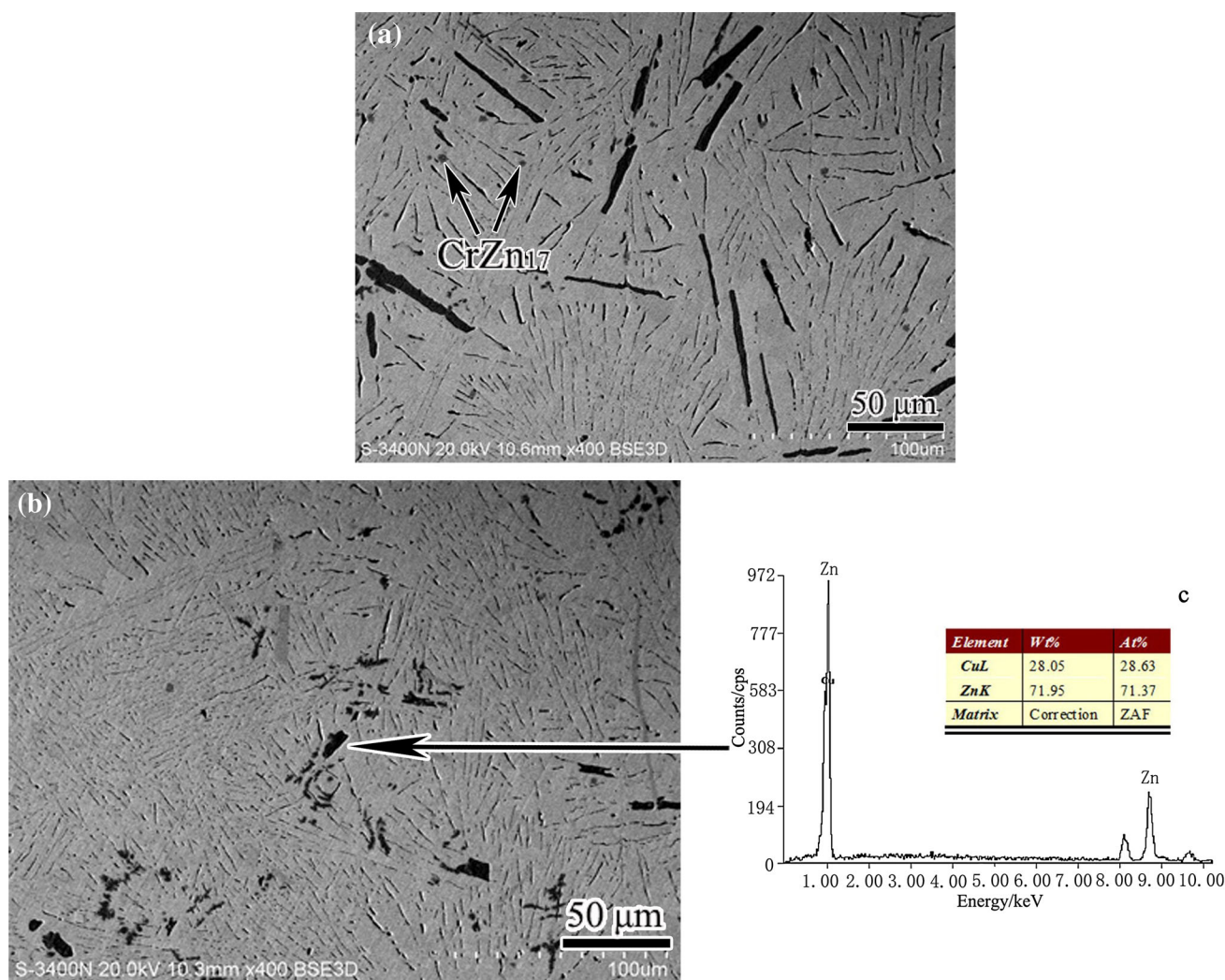


Fig. 4. Microstructure and EDS of SZC-xCu alloys: (a) SZC-0.05Cu and (b) SZC-0.1Cu.

validity. This is the reason why Cr addition can improve the antioxidant properties of the Sn-8.5Zn alloy. As shown in Table III, Nd and Al are surface-active elements which easily spread to the surface of the melting alloy. However, adding Nd or Al has opposite results. Addition of Al element can improve the antioxidant properties of SZC alloy. This is due to the fact that Al element combines with oxygen to generate a compact alumina film, preventing contact of the alloy liquid with air. In Table II, the antioxidant property of SZC-0.05Al alloy is better than that of SZC-0.1Al alloy, because the higher Al content results in formation of a thick alumina film, increasing the weight with oxide. It has been reported that Nd element can improve the antioxidant property of Sn-Zn alloy,¹⁸ but the result obtained in this work is somewhat different. According to the surface gloss experiments, the neodymium oxide film

was coarse with poor density. Meanwhile, the TGA results also showed that the SZC-Nd alloys were significantly heavier. This reveals that neodymium oxide film cannot prevent spread of oxygen, and accumulation of the active element Nd exacerbates oxidation of the Sn-Zn alloy. Zhou et al.⁵ also considered that solely adding Nd element to Sn-Zn alloy played no positive role in the antioxidant property. As shown in Table II and Fig. 6, addition of Cu element also could improve the antioxidant property of SZC alloy, even though the electronegativity difference between Cu and O is smaller than that between Zn and O. Because addition of Cu element can combine dissociated Zn in Sn-Zn alloy, the rate of diffusion of Zn atoms is reduced. Lee et al.⁹ confirmed that incorporation of Cu into Sn-Zn alloy is effective for improvement of oxidation resistance.

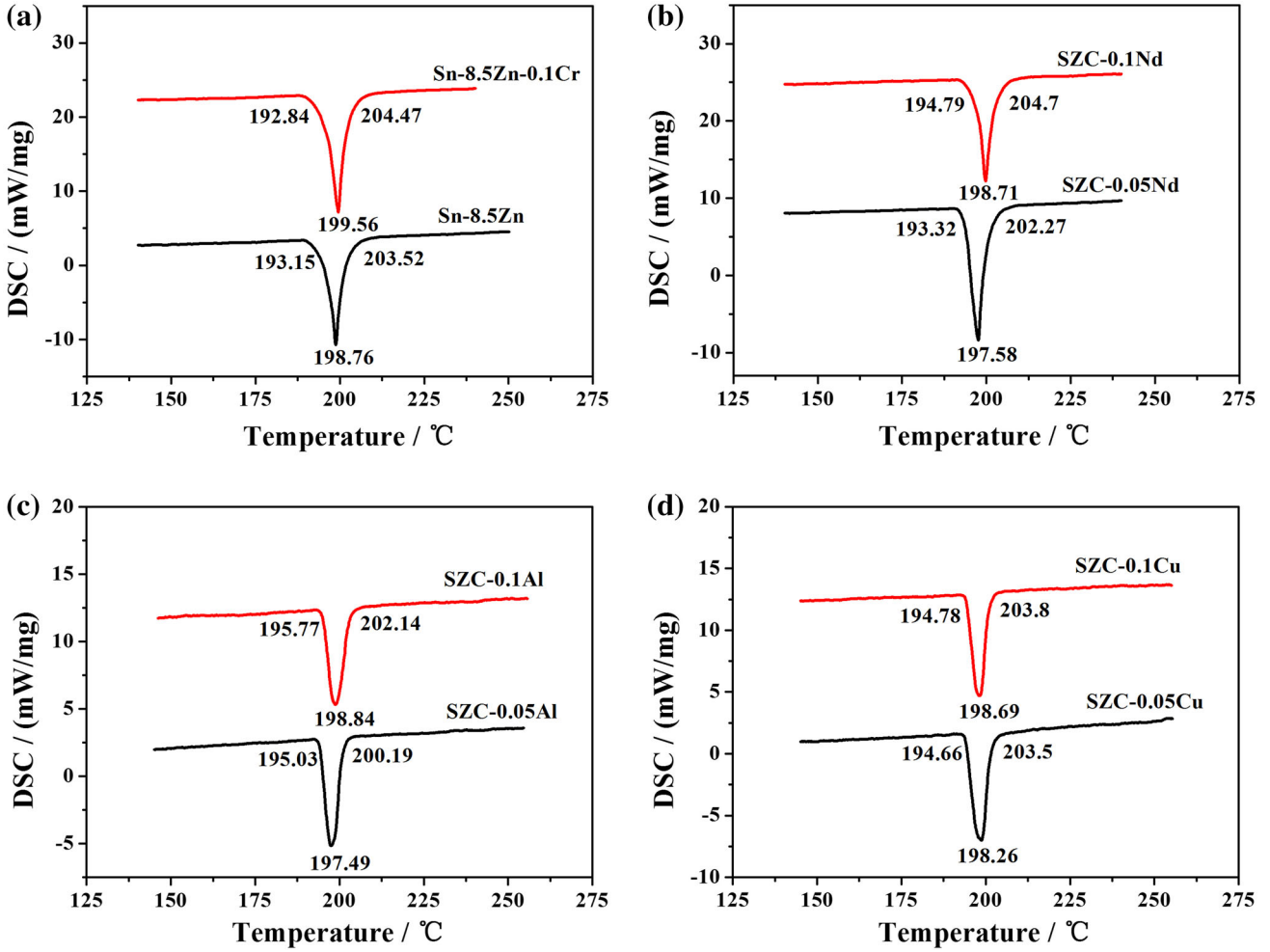


Fig. 5. DSC curves for SZC-xM alloys: (a) Sn-8.5Zn and SZC, (b) SZC-Nd, (c) SZC-Al, and (d) SZC-Cu.

Table I. DSC analysis results of SZC-xM alloys

Alloy	T_{onset} (°C)	T_{peak} (°C)	T_{end} (°C)	Melting range (°C)
Sn-8.5Zn	193.15	198.76	203.52	10.37
SZC	192.84	199.56	204.47	11.63
SZC-0.05Nd	193.32	197.58	202.27	8.95
SZC-0.1Nd	194.79	198.71	204.7	9.91
SZC-0.05Al	195.03	197.49	200.19	5.16
SZC-0.1Al	195.77	198.84	202.14	6.37
SZC-0.05Cu	194.66	198.26	203.50	8.84
SZC-0.1Cu	194.78	198.69	203.80	9.02

Wetting Behavior of Sn-Zn-Cr-M Alloys

In the spreading test, the wetting angle and spreading rate are the main parameters. The spreading rate test method was proposed in Japanese industrial standard JISZ3197. The spreading rate is represented as follows:

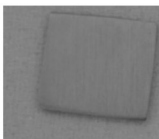
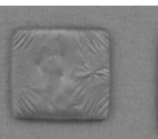
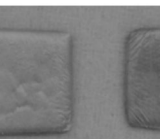

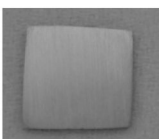
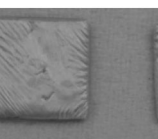
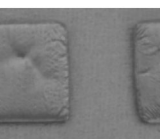
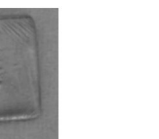
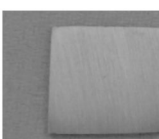
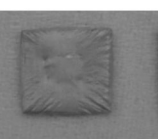
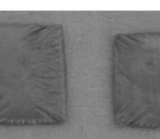

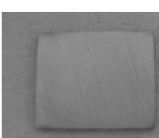
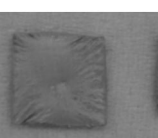
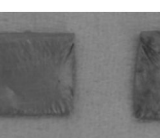

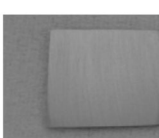
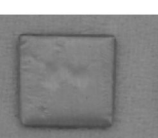
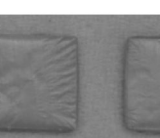
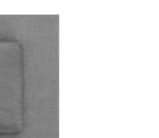
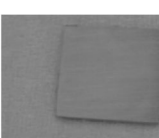
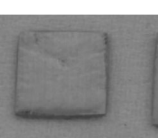
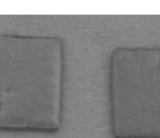

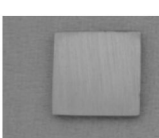
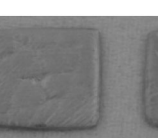
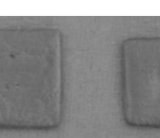

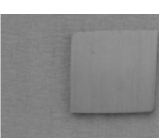
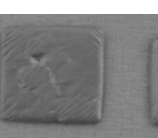
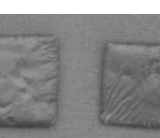

$$S = \frac{D-h}{D} \times 100\% \quad D = \sqrt[3]{\frac{6m}{3.14\rho}} \quad (1)$$

According to the geometrical relationship, the wetting angle can be calculated approximately as follows:

$$\theta = \sin^{-1} \frac{4dh}{d^2 + 4h^2}, \quad (2)$$

where D , h , m , ρ , and d represent the solder ball equivalent diameter, the average solder joint height, the quantity of solder, the density of solder,

Table II. Appearance of alloys after different heating times at 250°C

Alloy	Oxidation time				Compared with Sn-8.5Zn alloy
	0 h	1 h	24 h	72 h	
Sn-8.5Zn					-
SZC					Good
SZC-0.05Nd					Bad
SZC-0.1Nd					Bad
SZC-0.05Al					Excellent
SZC-0.1Al					Good
SZC-0.05Cu					Good
SZC-0.1Cu					Good

and the chord length of the solder joint spherical cap, respectively. S and θ represent the spreading rate and wetting angle. To calculate the spreading rate on Cu substrate, the solder density was measured in this work, as shown in Table IV.

As listed in Table IV, the wetting angle and spreading rate became more favorable with addition of Nd, Al or Cu. There are two reasons for the poor wettability of Sn-Zn alloy: First, the atoms are quite active and prone to oxidation; Second, Zn oxide is too loose to prevent further oxidation. In physics, low-surface-tension components gather easily at the surface of solution, which can reduce the surface energy of solution and allows the alloy to show positive adsorption.^{18,19} Nd is a surface-active element and has low surface tension, therefore Nd addition can significantly improve the wettability of SZC alloy. When the Nd content reached 0.1 wt.%, the wettability of the alloy reduced. This is due to

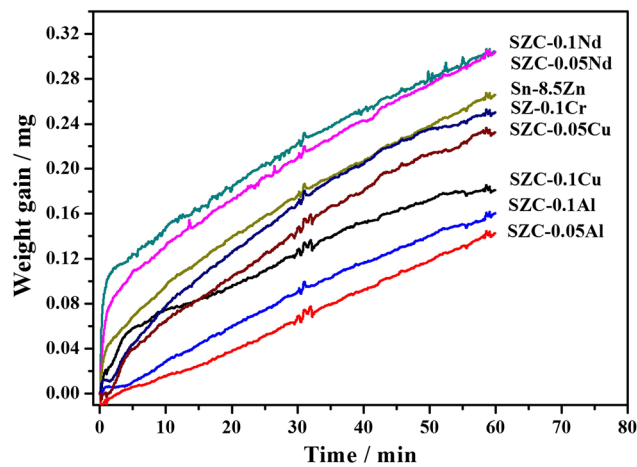


Fig. 6. TGA curves for Sn-8.5Zn alloy with added elements Cr, Nd, Al, and Cu.

the increasing amount of Nd that diffuses to the alloy surface, intensifying solder oxidation. Adding Al element can optimize the wettability, which is attributed to the antioxidant effect of Al element, in which a compact alumina film prevents Zn atoms from diffusing to the surface. When the Al content reached 0.1 wt.%, the wettability of the alloy also reduced. The main reason is that the increasing amount of Al results in thicker alumina film, weakening the liquidity of the alloy liquid. Cu addition can result in refinement or even disappearance of the long stripes of Zn-rich phase. With increasing Cu content, Cu-Zn intermetallic compounds are obtained, which greatly reduce the activity of Zn atoms. As listed in Table IV, as the Cu content was increased, the wettability of the alloy was monotonically enhanced. The wettability of the solder is related to the size of its microstructure. Fine and uniform microstructure can promote formation of precursor film in the spreading process, which is advantageous for solder wettability. This represents further favorable evidence that addition of Nd, Al or Cu can improve the wettability of SZC alloy, as shown in Figs. 1, 2, 3, and 4.

Table V. Microhardness of SZC-xM alloys

Alloy	Microhardness (HV)
Sn-8.5Zn	18.21
SZC	18.51
SZC-0.05Nd	19.03
SZC-0.1Nd	19.29
SZC-0.05Al	18.78
SZC-0.1Al	18.89
SZC-0.05Cu	18.75
SZC-0.1Cu	19.34

Table III. Electronegativity difference between some elements and oxygen

Element	La	Ce	Nd	Al	Cr	Zn	Cu	Sn	Pb
Electronegativity difference	2.33	2.32	2.3	1.83	1.78	1.79	1.54	1.48	1.11

Table IV. Density value, wetting angle, and spreading rate for SZC-xM alloys

Alloy	Density (g cm^{-3})	Wetting angle ($^{\circ}$)	Spreading rate (%)
Sn-8.5Zn	7.301	39.3	56.89
SZC	7.288	38.3	58.07
SZC-0.05Nd	7.249	35.7	60.26
SZC-0.1Nd	7.238	35.9	60.13
SZC-0.05Al	7.218	36.3	59.93
SZC-0.1Al	7.172	36.6	59.24
SZC-0.05Cu	7.308	36.9	59.21
SZC-0.1Cu	7.317	36.5	59.38

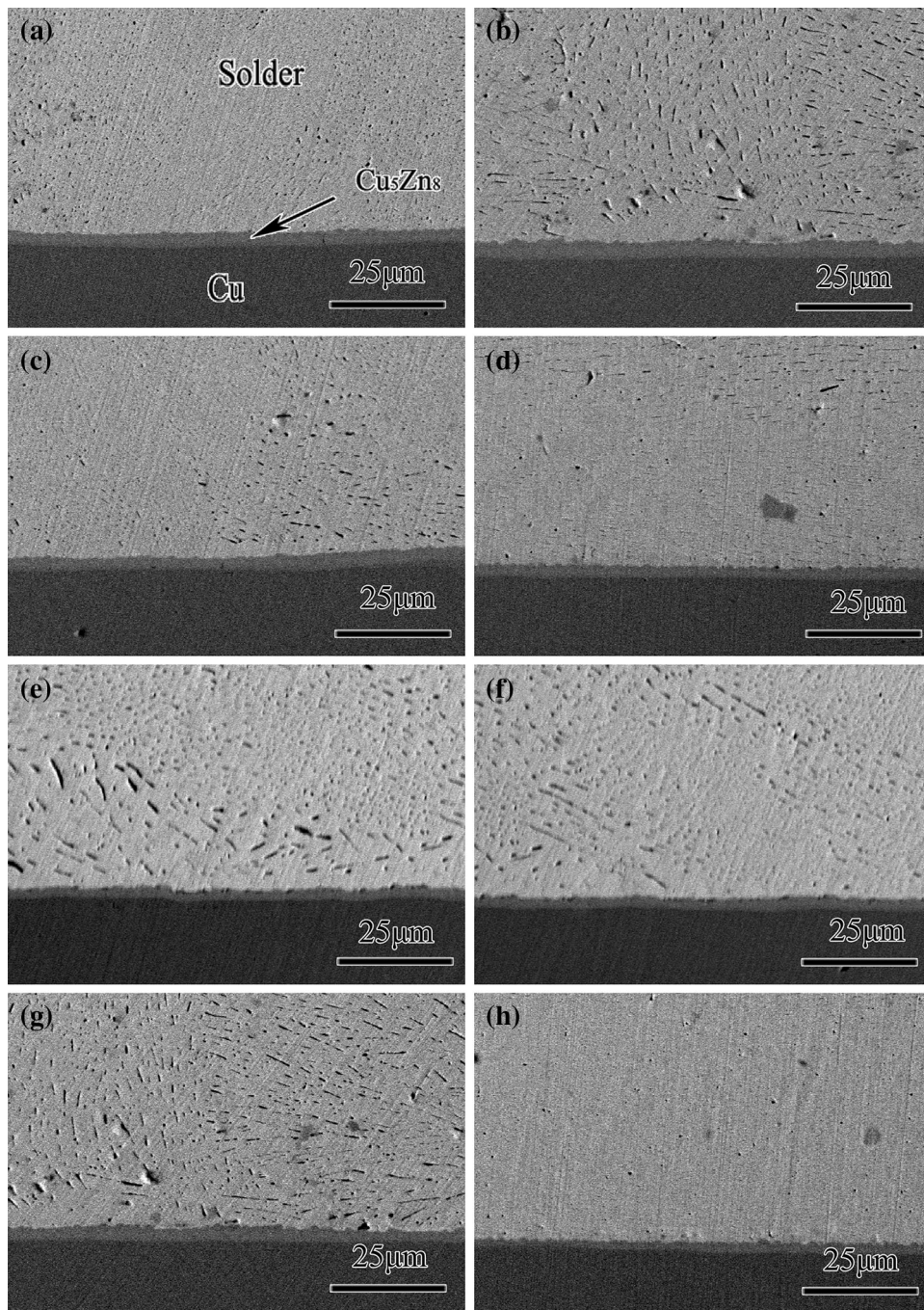


Fig. 7. Interface morphology of SZC-xM/Cu: (a) Sn-8.5Zn/Cu, (b) SZC/Cu, (c) SZC-0.05Nd/Cu, (d) SZC-0.1Nd/Cu, (e) SZC-0.05Al/Cu, (f) SZC-0.1Al/Cu, (g) SZC-0.05Cu/Cu, and (h) SZC-0.1Cu/Cu.

Microhardness Behavior of Sn-Zn-Cr-M Alloys

The microhardness results for the alloys are presented in Table V. The microhardness of the Sn-8.5Zn alloy was 18.21 HV, and the microhardness of the solder alloy was improved with alloying element addition. On addition of Cr element, the microhardness of Sn-8.5Zn alloy was increased to 18.51 HV. When the content of Cr was 0.1 wt.%, not

only was the alloy microstructure refined, accompanied by fine grain strengthening, but a second phase was also generated, resulting in second phase strengthening. When Nd, Al or Cu element was added to Sn-8.5Zn-0.1Cr alloy, the microhardness also increased with increasing alloying element content. This is because the stripes of Zn-rich phase in Sn-Zn alloy are brittle and easily lead to stress

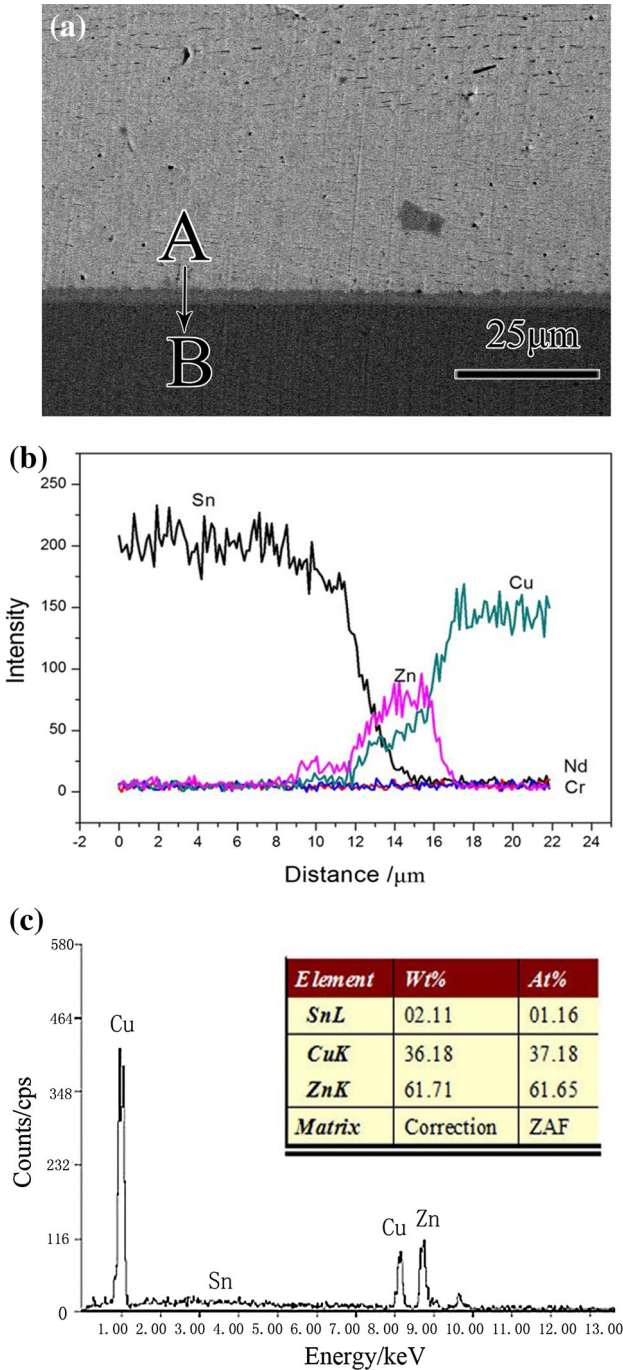


Fig. 8. Interface analysis of SZC-0.1Nd/Cu: (a) interface morphology, (b) line scan from point A to B, and (c) energy spectrum of interface.

concentration under strain. Considering the microstructure, addition of alloying elements would refine the stripes of Zn-rich phase in the solder alloy, make the microstructure more uniform, and refine the eutectic structure (Figs. 1, 2, 3, and 4), while simultaneously increasing grain boundaries and dislocations, so that the microhardness of the alloy would increase.

Interface Morphologies of Sn-Zn-Cr-M/Cu

The cross-sectional morphologies of SZC-*x*M/Cu interfaces without aging are illustrated in Fig. 7. As shown in Fig. 7, the intermetallic layer morphologies are almost the same, revealing a continuous and flat type. According to EDS analysis (Fig. 8), the intermetallic layer was Cu_5Zn_8 but no Cu–Sn phase was formed. The reason is that the higher activation energy barrier for nucleation makes Cu–Sn phase formation difficult.

The intermetallic layer thickness of the SZC-*x*M/Cu interfaces is listed in Table VI. The average IMC thickness for Sn-8.5Zn/Cu and SZC/Cu was 3.09 μm and 3.04 μm . With addition of Nd, Al or Cu, the IMC layer was slightly thinner. This suggests that addition of Nd, Al or Cu is conducive to solder joint reliability, because the interface reaction layer is brittle, and the thermal expansion coefficient is very different for the solder substrate and IMC layer. Addition of Nd, Al or Cu can refine the microstructure of the SZC alloy, particularly refining the long stripes of Zn-rich phase, and can promote precipitation of CrZn_{17} phase to reduce the activity of Zn element. During soldering, Nd and Al elements easily gather in the interface between solder and Cu substrate, preventing diffusion of Zn atoms. When the Cu content was 0.1 wt.%, the IMC layer thickness reduced to 2.5 μm . It was observed that, when the Cu content was 0.1 wt.%, the Zn-rich phase basically disappeared and the Cu_5Zn_8 phase was found in the microstructure, preventing diffusion of Zn atoms.

Figure 9 shows the interface microstructure evolution in SZC-*x*M/Cu after isothermal aging treatment at 150°C for 15 days. Figure 10 shows EDS analysis of the SZC-0.1Nd/Cu interface after 15 days of aging; the IMC at the interface was determined to be Cu_5Zn_8 . As shown in Fig. 9a and b, the Sn-8.5Zn/Cu and SZC/Cu interface layer obviously thickened (16.35 μm and 15.77 μm , respectively), and the continuous Cu–Zn interface layer

Table VI. Interface layer thickness of SZC-*x*M alloys before and after aging. (a) Sn-8.5Zn/Cu, (b) SZC/Cu, (c) SZC-0.05Nd/Cu, (d) SZC-0.1Nd/Cu, (e) SZC-0.05Al/Cu, (f) SZC-0.1Al/Cu, (g) SZC-0.05Cu/Cu, and (h) SZC-0.1Cu/Cu

Aging condition	IMC thickness (μm)							
	a	b	c	d	e	f	g	h
Before aging (Fig. 5)	3.09	3.04	2.70	2.65	2.35	2.26	2.85	2.50
After aging for 15 days at 150°C (Fig. 7)	16.35	15.77	15.00	15.39	10.39	12.50	15.57	12.51

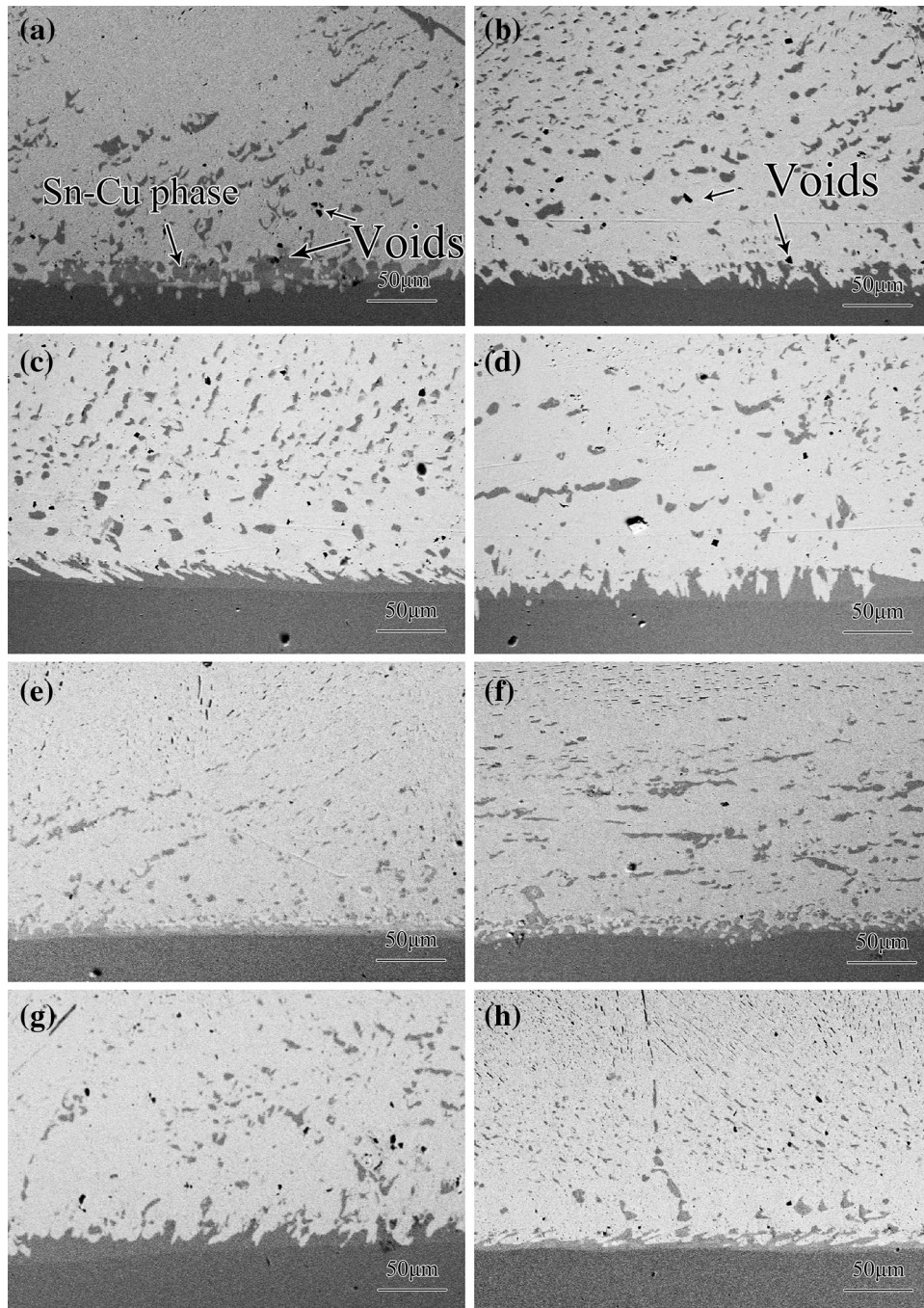


Fig. 9. Interface morphology of SZC-xM/Cu after aging for 15 days: (a) Sn-8.5Zn/Cu, (b) SZC/Cu, (c) SZC-0.05Nd/Cu, (d) SZC-0.1Nd/Cu, (e) SZC-0.05Al/Cu, (f) SZC-0.1Al/Cu, (g) SZC-0.05Cu/Cu, and (h) SZC-0.1Cu/Cu.

was severely destroyed. At the same time, Cu-Sn compounds formed between the Cu substrate and Cu-Zn interface layer, accompanied by void formation. Such a discontinuous interface layer and voids adversely affect solder joint reliability.

During aging, some small-size Cu_5Zn_8 phase formed in the bulk solders, and these scattered Cu_5Zn_8 phases grew and increased with extending aging time. During long-term aging, Zn atoms continuously diffuse to the interface, leading to

increased thickness of the interface layer, while Cu atoms also diffuse into the solder substrate, then dissociated Zn combines with Cu to form Cu_5Zn_8 compound. A unique area was found in the solder substrate, called a Zn-poor or transition layer²⁰ because of the decrease of dissociated Zn. This transition layer expands with extending aging time, and its thickness can exceed 200 μm after 15 days of aging. With addition of Nd, Al or Cu, the thickness of the transition layer decreased, improving the

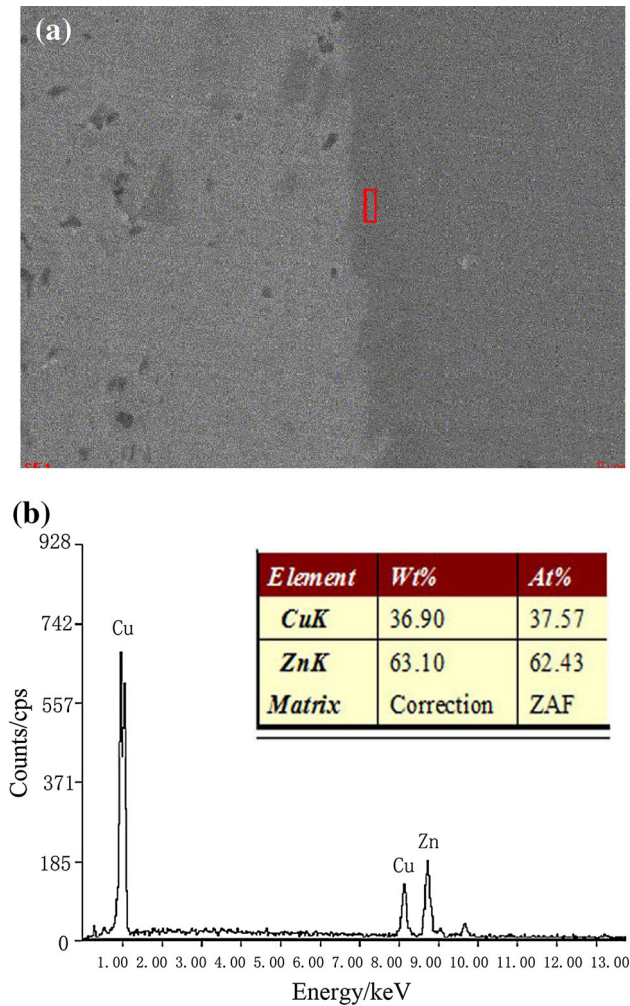


Fig. 10. Interface analysis of SZC-0.1Nd/Cu after aging at 150°C for 15 days: (a) interface morphology and (b) energy spectrum of interface.

solder joint reliability, because large bulk Cu_5Zn_8 phases are brittle and can easily cause stress concentration under service conditions.

As shown in Table VI, with addition of Nd, Al or Cu, the IMC interface layer also thickened obviously and the interface morphology became uneven, albeit remaining much thinner than for the Sn-8.5Zn/Cu and SZC/Cu interfaces. After 15 days of aging, the thickness of the SZC-0.05Nd/Cu and SZC-0.1Nd/Cu interfaces was 15 μm and 15.39 μm . The reason is that the fine grains increase the number of grain boundaries and increase the barriers that the elements must overcome in order to diffuse. Zeng et al.²¹ reported that Nd element can limit diffusion of Sn atoms during aging, avoiding generation of more bulky Sn-Cu phase. The thickness of the SZC-0.05Al/Cu and SZC-0.1Al/Cu interfaces was 12.50 μm and 10.39 μm , being thinner than the other alloys' interfaces. Besides grain refinement, this is also associated with the surface activity of Al element. Lin and Liu²² confirmed that a thin layer

of Al-Zn-Cu compounds was found at the side of the interface near the Cu substrate, which slowed down mutual diffusion of elements. In this work, an obvious Al-Zn-Cu layer was not detected, but the role of Al element in hindering mutual diffusion is indisputable. The thickness of the SZC-0.05Cu/Cu and SZC-0.1 Cu/Cu interfaces was 15.57 μm and 12.51 μm . When the content of Cu was 0.05 wt.%, the long stripe Zn-rich phases became short rods, with Cu atoms mainly existing in solid-state form. Therefore, diffusion of Zn atoms was not obviously limited. When the Cu content was 0.1 wt.%, the long stripe Zn-rich phases basically disappeared, while some small-size Cu_5Zn_8 phases were found. Meanwhile, the concentration gradient of Cu between the Cu substrate and solder was reduced. So, the thickness of the SZC-0.1Cu/Cu interface was significantly less than that of the SZC-0.05Cu/Cu interface.

CONCLUSIONS

Nd, Al or Cu element addition not only altered the microstructure but also affected the properties of SZC alloy. The following conclusions can be drawn:

1. Addition of Nd, Al or Cu element significantly refined the microstructure of SZC alloy, especially promoting disappearance of the stripe Zn-rich phase. Secondary phases were found in the alloys when the addition reached 0.1 wt.%. NdSn_3 in SZC-0.1Nd alloy, Al-Zn phases in SZC-0.1Al alloy, and dispersed and granular Cu_5Zn_8 in SZC-0.1Cu alloy.
2. Addition of Nd, Al or Cu element significantly improved the melting characteristics, wettability, and microhardness of SZC alloy. Addition of Al or Cu element improved the oxidation resistance of SZC alloy, while the alloys were obviously oxidized on addition of rare-earth element Nd. In other words, Nd element reduced the oxidation resistance of SZC alloy.
3. SZC- $x\text{M}$ /Cu interfaces without aging were thin and flat, being neither obviously concave nor convex. The intermetallic layer composition was recognized as Cu_5Zn_8 phase by EDS analysis. After 15 days of aging, the Sn-8.5Zn/Cu interface thickened obviously and was severely damaged. A wide Zn-poor or transition zone was found in the solder. The IMC growth rate was reduced after microalloying, and the transition zone narrowed. Therefore, with addition of Nd, Al or Cu element, the thermal stability of the welding interface was increased.

ACKNOWLEDGEMENTS

This research work is jointly supported by the Guangxi Science and Technology Development Project (11107003-1, 12118001-2B, 2013AA01013), the Science and Technology Project of Guangxi

Education Department (2013ZL010), the Science and Technology Development Project of Qingxiu District, Nanning (2013S08), and Middle-aged and young teachers in colleges and universities in Guangxi basic ability promotion project (KY2016YB022).

REFERENCES

1. M.N. Islam, Y.C. Chan, M.J. Rizvi, and W. Jillek, *J. Alloys Compd.* 400, 136 (2005).
2. X. Chen, A. Hu, M. Li, and D. Mao, *J. Alloys Compd.* 460, 478 (2008).
3. Y.H. Hu, S.B. Xue, H. Wang, H. Ye, Z.X. Xiao, and L.L. Gao, *J. Mater. Sci. Mater. Electron.* 22, 481 (2010).
4. Y.H. Hu, S.B. Xue, H. Ye, Z.X. Xiao, L.L. Gao, and G. Zeng, *Mater. Des.* 34, 768 (2012).
5. J. Zhou, D. Huang, F. Xue, Y.S. Sun, and P.P. Li, China patent B23K 35/26 (P) (9 July 2008).
6. S.K. Das, A. Sharif, Y.C. Chan, N.B. Wong, and W.K.C. Yung, *J. Alloys Compd.* 481, 167 (2009).
7. A. Kantarcioğlu and Y.E. Kalay, *Mater. Sci. Eng. A* 593, 79 (2014).
8. H. Wang, S. Xue, F. Zhao, and W. Chen, *J. Mater. Sci. Mater. Electron.* 21, 111 (2009).
9. J.E. Lee, K.S. Kim, M. Inoue, J. Jiang, and K. Suganuma, *J. Alloys Compd.* 454, 310 (2008).
10. D.Q. Yu, H.P. Xie, and L. Wang, *J. Alloys Compd.* 385, 119 (2004).
11. X. Chen, A. Hu, M. Li, and D. Mao, *J. Alloys Compd.* 470, 429 (2009).
12. J. Hu, A. Hu, M. Li, and D. Mao, *Mater. Charact.* 61, 355 (2010).
13. T.B. Luo, A.M. Hu, J. Hu, M. Li, and D.L. Mao, *Microelectron. Reliab.* 52, 585 (2012).
14. J.Q. Cai, *Print. Circuit Inf.* 5, 61 (2006).
15. C.M.L. Wu and Y.W. Wong, *J. Mater. Sci. Mater. Electron.* 18, 77 (2006).
16. A. Sebaoun, D. Vincant, and D. Treheux, *Mater. Sci. Technol.* 3, 241 (1987).
17. N. Huang, A.M. Hu, M. Li, and D. Mao, *J. Mater. Sci. Mater. Electron.* 24, 2812 (2013).
18. J. Zhou, D. Huang, Y.L. Fang, and F. Xue, *J. Alloys Compd.* 480, 903 (2009).
19. C.M.L. Wu, D.Q. Yu, C.M.T. Law, and L. Wang, *J. Electron. Mater.* 32, 63 (2003).
20. K. Suganuma, K. Niihara, T. Shoutoku, and Y. Nakamura, *J. Mater. Res.* 13, 2859 (1998).
21. G. Zeng, S. Xue, L. Gao, L. Zhang, Y. Hu, and Z. Lai, *J. Alloys Compd.* 509, 7152 (2011).
22. N.S. Liu and K.L. Lin, *J. Alloys Compd.* 456, 466 (2008).